Title: Periodic Time Cells in Human Entorhinal Cortex

Authors: Zahra M. Aghajan [1], Gabriel Kreiman [2,3], Itzhak Fried [1,4,5,*]

Affiliations:

[1] *Department of Neurosurgery, David Geffen School of Medicine, University of California Los Angeles, Los Angeles, CA.*
[2] *Children's Hospital, Harvard Medical School, Boston, MA, USA.*
[3] *Center for Brains, Minds and Machines, Massachusetts Institute of Technology, Cambridge, MA, USA.*
[4] *Department of Psychiatry and Biobehavioral Sciences, Jane and Terry Semel Institute for Neuroscience and Human Behavior, University of California Los Angeles, Los Angeles, CA.*
[5] *Tel Aviv Medical Center and Sackler School of Medicine, Tel Aviv University, Tel Aviv, Israel.*

*Correspondence to: ifried@mednet.ucla.edu

Abstract:
The representation of time in the brain is a fundamental component of cognition. Here we investigated how the human brain represents time during a temporally continuous uninterrupted experience by presenting fifteen neurosurgical patients with an audiovisual video while recording neurons' activity from multiple brain regions. We report on a set of units that modulate their activity in a strikingly periodic manner across different timescales—from seconds to many minutes. These cells were most prevalent in the entorhinal cortex and time could be decoded from their population activity. Furthermore, these cells remapped their dominant periodicity to shorter timescales during a subsequent recognition memory task. When the audiovisual sequence was presented at two different speeds (regular and faster), a significant percentage of these periodic time cells (PTCs) maintained their timescales, suggesting a degree of invariance with respect to the narrative content. The temporal periodicity of PTCs may complement the spatial periodicity of grid cells, thereby providing scalable spatiotemporal metrics for encoding and retrieval of human experience.

Introduction:

Episodic memories integrate the content of human experience in space and time and constitute the basis for our remarkable ability for mental time travel(*1–4*). In rodents, several temporal coding schemes involving the hippocampal-entorhinal circuitry have been reported(*5–14*), including: (a) "time cells" in the hippocampus and medial entorhinal cortex (MEC) firing at specific points in time during a short timed interval(*5–7*); (b) "ramping cells" in the lateral entorhinal cortex (LEC) whose ramping firing activity enables extraction of time for distinct experiences during the task(*14*); (c) "event-specific" cells in the hippocampus coding for temporal order of events(*12*); and (d) degradation in the population of place cells' activity over hours and days (*8–11*). Together, the firing properties of these cells—i.e., their sequential activation or their activity decay at different timescales—with respect to experimental temporal boundaries, are thought to provide timestamps of episodic memory.

Uncovering a neuronal code for the representation of time in the human hippocampal-entorhinal system is critical to shed light on the temporal mechanisms of memory formation. In stark contrast to real life, most lab-based episodic memory experiments are often dominated by a stimulus-response methodology—requiring intermittent sensory input and subject response—therefore, disrupting the natural temporal continuity of behavior. Understanding how time is encoded, however, requires a more naturalistic scenario where time is studied at multiple timescales over prolonged periods spanning seconds to many minutes.

To approach the fundamental question of temporal representation in the human hippocampal-entorhinal system, one can adopt a framework that regards time as an additional dimension to space. In analogy with "grid cells" in the entorhinal cortex providing a scalable map with spatial periodicity(*15*, *16*), we hypothesize that cells in human entorhinal cortex would provide a scalable map of time with periodic properties. If such a temporal map existed, one would expect that spatial grid properties—such as rate remapping (as a result of environmental changes) and distinct grid modules with different spatial scales—would translate into the time domain. Indeed, this hypothesis is consistent with recent accounts on the role of rodent MEC in interval timing and the idea of "navigating through time" (*17–19*).

We sought to investigate the existence of a periodic time code that can provide multiple timescales for human experience. We created a realistic immersive flow of information along extended temporal scales—by employing a paradigm with uninterrupted audiovisual sequence—while we recorded units' activity in multiple brain regions in humans.

Results:

<u>Behavioral task</u>

Participants were fifteen neurosurgical patients (age = 33±10; 9 Female) with intractable epilepsy who were implanted with intracranial depth electrodes in order to identify the seizure focus for potential subsequent surgical cure. First, we recorded spiking activity from microwires while ten of the fifteen participants watched a 42-minute movie (first episode, season six of "24" TV series; Fig. 1a)(*20*) and performed a recognition memory test afterwards. During the memory test, they were presented with brief movie shots and were asked whether they had seen the clip before. The target movie shots were randomly interleaved with an equal number of foil movie shots (chosen from the second episode of "24" that the patient had not seen, Fig. 1a, b; for further detail see Methods, Behavioral Tasks).

Presence of units with periodic modulation of firing in time

We identified 537 units with a minimum firing rate of 0.05Hz (mean rate = 0.93, [0.28, 3.85] Hz) using previously described methods(*21–24*) (Methods, Data Acquisition). In order to localize these units for each participant, a high-resolution post-operative CT image was co-registered to a pre-operative whole brain and high-resolution MRI and the location of the microwires were determined for each depth electrode (Fig. 1c; Methods, Electrode Localization). These units were thus localized to eleven unique regions (Table S1) with more than half of the units (52.32 %) recorded from MTL regions (Table S2). To display the firing rate of each unit, we binned the spikes into 100ms segments and applied a Gaussian smoothing kernel with 500ms width, followed by division by the duration of the time bin (Fig. 2a; Methods, Electrophysiological Analyses). Visual examination of the firing rates revealed that some units exhibited striking periodicity in their firing over the course of the movie, and the timescale of this periodicity varied from unit to unit, ranging from tens of seconds to several minutes (Fig. 2a). This periodicity was further demonstrated by the peaks observed in the autocorrelogram of each unit's firing rate in time (Fig. 2b; Methods, Electrophysiological Analyses). Additionally, we used Generalized Linear Models (GLMs) to model the time-varying firing rate as a Poisson process using basis functions that were periodic in time and inspected the model fit as well as the basis functions that were significant in explaining the rate (Fig. 2a, Fig. S1; Methods, Electrophysiological Analyses). The firing rate of these cells oscillated with a periodicity centered around one or more characteristic frequency. We refer to these cells as Periodic Time Cells (PTC) given that their firing rate appears periodic in time.

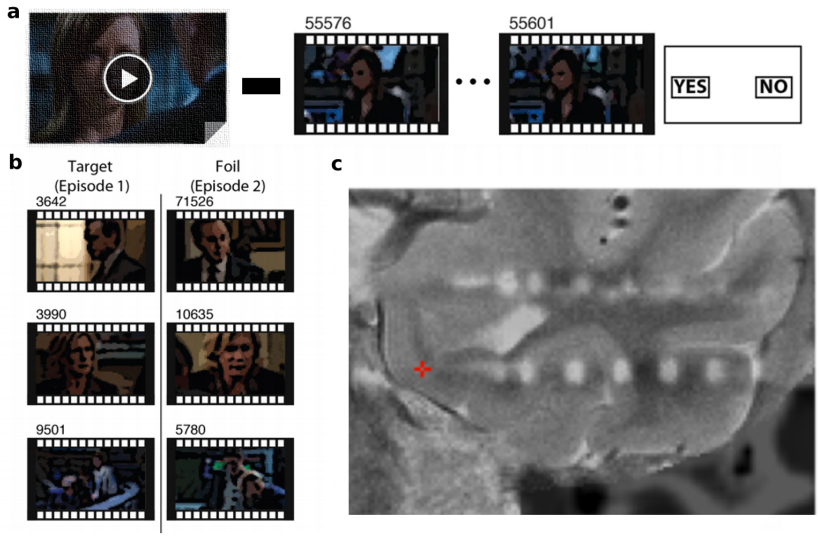

Figure 1: Task structure and electrophysiological recordings. a. Participants watched an episode of the 24 series (~42 minutes in duration) and afterwards they were tested for recognition memory where they were shown short clips and asked whether they had previously seen them. **b.** The memory test included target clips (taken from the same episode they had watched, left column) and foil clips (taken from the next episode they had never seen before, right column). Images are adapted and modified from a previous publication(*20*). **c.** Depth electrodes were localized by co-registering high resolution post-operative CT images with high resolution preoperative MRI. Red crosshair indicates the location of a microwire in the left entorhinal cortex.

To quantitatively assess the extent to which neurons fired in a periodic fashion, we computed the autocorrelation of the firing rate for each unit and compared it against the null hypothesis constructed using shuffled data (specifically, the autocorrelations computed over the shuffled firing rates of the same unit; for details see Methods, Electrophysiological Analyses). A unit with an autocorrelation values outside the [2.5%, 97.5%] of the shuffled data was identified as a putative PTC. Furthermore, we used a cluster-based permutation test to correct for multiple comparisons in identifying these units and found a total of 114 PTCs (Fig. S2a; more examples of PTCs are shown in Fig. S3). We then quantified the percentage of PTCs within each region and found that multiple regions contained a significant fraction of these units, with the entorhinal

cortex holding the largest population of PTCs (42 out of 122 total entorhinal units; 34.43%, [26.06, 43.57]%, confidence intervals from binomial test), followed by the parahippocampal region (8 out of 27 total parahippocampal units; 29.63%, [13.75, 50.18]%, confidence intervals from binomial test)(Fig. 2c, Table S2).

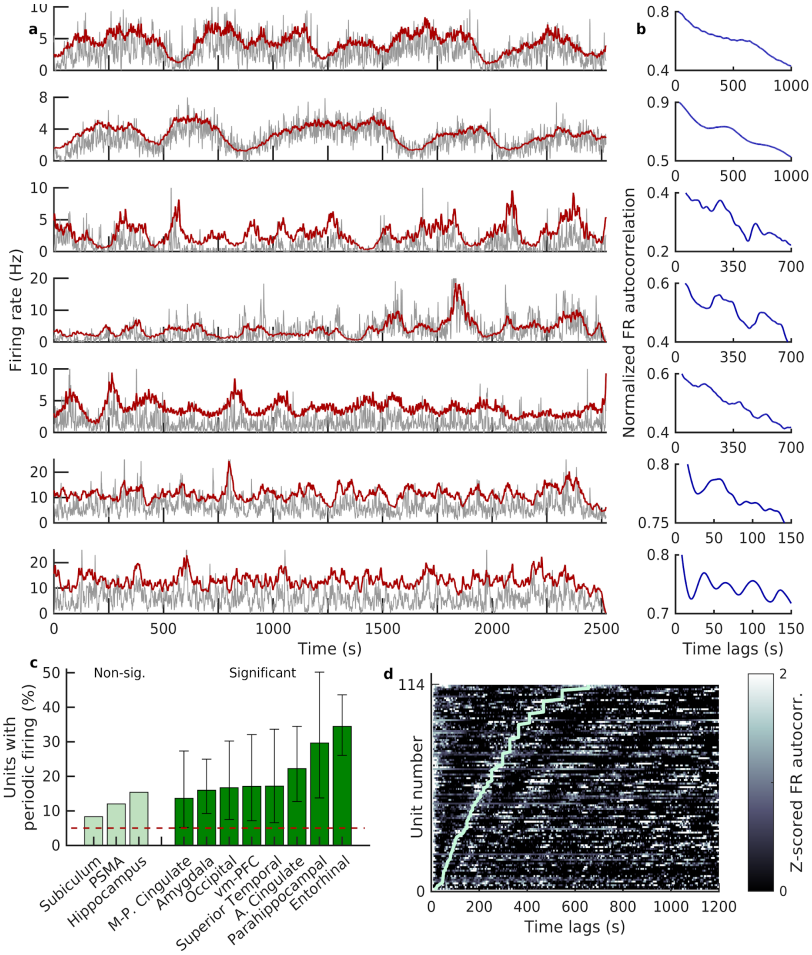

Figure 2: Periodic Time Cells (PTCs) exhibited significant periodic firing during movie viewing. **a.** Seven example PTCs firing activity. These units were recorded from ventromedial prefrontal cortex (vm-PFC), entorhinal cortex (EC), EC, anterior cingulate, EC, EC, and parahippocampal gyrus respectively. Gray line indicates the firing rate (smoothed spike train divided by the 100ms time bin). Red line indicates the GLM fitted firing rate (see Methods). **b.** Each row is the normalized autocorrelation of the smoothed firing rate of the unit shown in (a). Note the local peaks in the autocorrelograms (showing a periodicity in the unit firing), as well as the different timescales for each unit (x-axis limits are adjusted according to the unit's timescale). The autocorrelations are smoothed only for visualization purposes. **c.** Within each recording region, the percentage of PTCs during movie viewing are shown in green bars and the error bars indicate the confidence intervals of a binomial test (for a full list of the number of recorded units and significant PTCs per region, see Table S2). The EC region had the largest percentage of PTCs and the regions marked in light green did not have a significant percentage of PTCs (the confidence intervals of the binomial test included the 5% chance level). **d.** Z-scored autocorrelations of all the PTCs' firing rate (colormap; N = 114) were sorted by the dominant periodicity (light green line, see Methods) for each unit (each row). Note the visible diverging lines parallel to the dominant period, corresponding to periodicity in the signal. The dominant periodicity of the units shown in (a) are as follows: 655.36s, 409.60s, 297.89s, 297.89s, 182.04s, 51.20s, 36.41s.

<u>PTCs' periodicities spanning multiple timescales</u>

We next asked how the periodicity of PTCs varied across units. We calculated the dominant period for each unit as follows: 1) the firing rate autocorrelation was z-scored with respect to the shuffled data for each unit; 2) an FFT was performed on the z-scored autocorrelation values; and 3) the period at which the largest power was contained was determined to be the dominant period for that unit (Fig. S2; Methods, Electrophysiological Analyses). This approach allowed us to examine the periodicity scale of all PTCs. The population activity of these units spanned temporal scales ranging from tens of seconds to several minutes (Fig. 2d). It is worth noting that such large temporal scales are beyond the temporal response patterns of traditional time cells, previously observed in the hippocampus and medial entorhinal cortex (MEC) of rodents, which involved temporal scales on the order of a few seconds(*6*, *7*). The timescales of PTCs are more similar to those of the ramping time cells discovered in the rodent LEC(*14*).

The population of PTCs exhibited multiple timescales even within each participant (Fig. 3a; Table S3), as well as within different regions (Fig. 3b). At the population level, the distribution of the PTCs' dominant periods revealed a non-uniform distribution ($p < 10^{-5}$; single sample Kolmogorov-Smirnov test against uniform distribution) and some timescales appeared to be more pronounced (e.g., dominant periodicities at 60.5s, 98.5s, 165.5s, 238s and 354s; Fig. 3c). To further investigate the presence of preferred timescales, we applied principal component analysis on the population of PTCs' firing rates (Methods, Electrophysiological Analyses). The eigenvectors themselves were periodic in time and their periodicity—similar to the results obtained from the autocorrelation analysis (Fig. 3c)—exhibited specific periods that were over-represented in the population (Fig. S4), further corroborating the presence of preferred timescales within the PTCs.

Although thus far the results focused on the dominant periodicity (the oscillation with the highest power), some units had periodic firing at additional temporal scales. To determine other prominent oscillations, we calculated the relative power of the z-scored firing rate autocorrelation with respect to the power at the dominant period and found the peaks with at least 75% of the maximum power (Fig. 3d). Indeed, 34.21% of the units showed periodic firing at one or more frequencies in addition to their dominant periodicity (Fig. 3e). These additional frequencies were not simply multiples of each other. Few units had more than two additional frequencies.

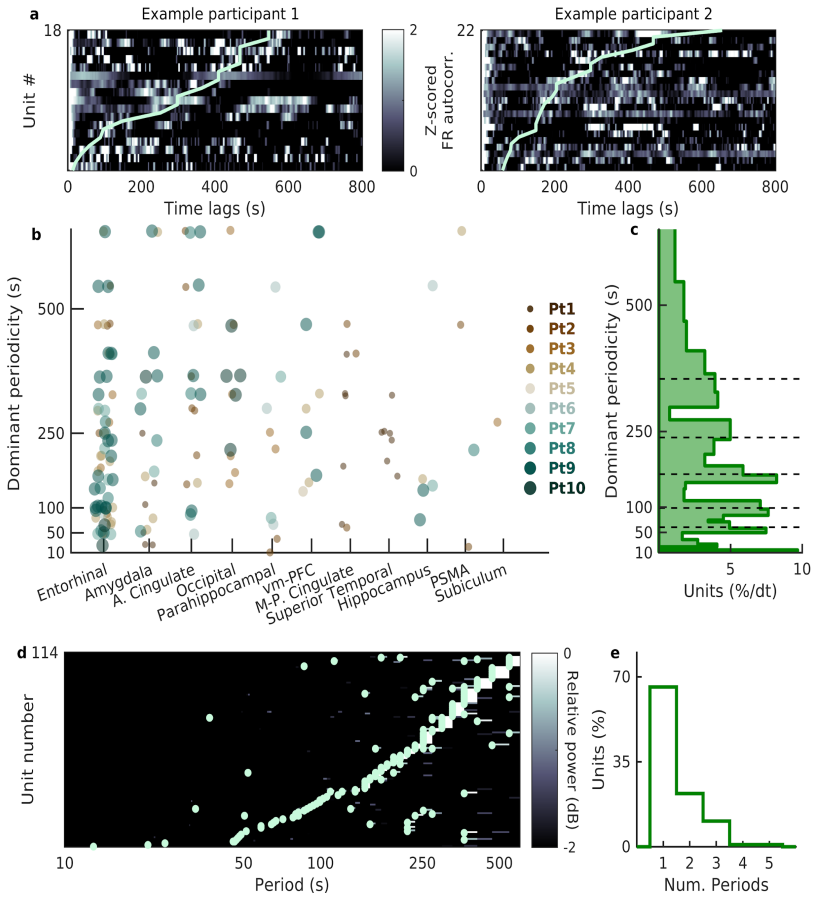

Figure 3: Distributions of the PTCs' timescales. a. Distributions within subjects**.** Z-scored autocorrelation of the PTCs' firing rates (colormap) for two example participants sorted by the dominant periodicity (light green line) for each unit (each row). **b.** Dominant periods of PTCs are shown within each region and for each participant (different colored/sized circles). **c.** The distribution of the dominant periodicity of all PTCs was not uniform ($p < 10^{-5}$; single sample Kolmogorov-Smirnov test against uniform distribution). Due to the non-uniform bins, the percentage of units in each bin is normalized by the duration of the time bin. Note the pronounced peaks at 60.5s, 98.5s, 165.5s, 238s and 354s (marked with dashed lines). **d.** To determine prominent oscillations at periods other than the dominant periodicity, we examined relative power of the z-scored auto- correlogram (with respect to the maximum power at the dominant periodicity) for each unit (row) sorted by the dominant period. Light green circles indicate periods at which power was at least 75% of the maximum power (corresponding to the dominant period). **e.** Using the method in (d), we found the number of prominent periods (including the dominant period) for each unit. Shown is the distribution of the number of periods per unit and 34.21% of the units had prominent periodic activity in addition to their dominant periodicity.

Decoding time from the PTCs' population activity

If the activity of the PTCs contained information about time, it should be possible to decode time from PTCs' population activity. To test this, we first partitioned the duration of the movie into equally sized epochs (bin durations for the epochs ranged from 1-90 seconds). We used linear discriminant analysis with a holdout approach to predict the time epoch within the movie using the firing rate of the PTCs as input features (Methods, Electrophysiological Analyses). We found that for bin durations longer than 5 seconds we were able to successfully decode time and the accuracy of the model, applied on an independent test set, was significantly above chance level (decoding time from shuffled PTCs' firing rates; Fig. 4). The ability to extract precise, localized, temporal information from the population of PTCs, but not the shuffled data, shows that the periodic activity of the PTCs constitutes a viable mechanism to encode time. How the hippocampus may integrate such temporal information and incorporate it into encoding and retrieval of episodic memories deserves further investigations(*25–27*).

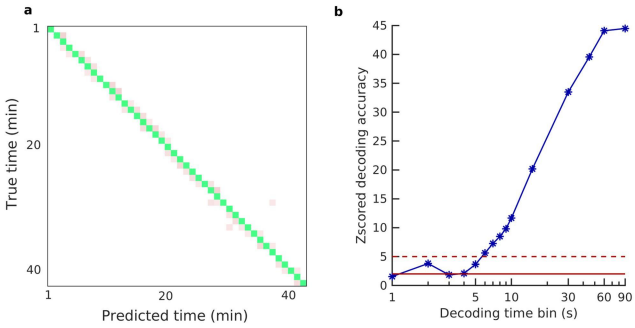

Figure 4. Decoding time from the population activity of the PTCs. a. Example confusion matrix (of the test set) from the time decoding analysis. Here, the time within the movie, and thus the activity of the PTCs (N=114), was divided into one-minute-long epochs and used as the input feature, while the output vector corresponded to the time bin numbers. Shown are the correctly classified time bins in green (the diagonal) and incorrectly classified time bins in pink (off diagonal). **b.** Decoding accuracy of the model on the test set was z-scored with respect to the shuffled data (decoding accuracy on shuffled PTCs' firing rates) for different decoding bin sizes. For epochs larger than 5 seconds in duration, decoding accuracy was significantly above chance level (z=5; red dashed line).

Invariance of PTCs' periodicities with respect to narrative content

Can the presence of periodicity in the firing activity of the neurons be explained by the particular events and structure of this movie? First, we asked whether the cuts in the movie—defined as consecutive frames between sharp transitions(*20*)—were responsible for eliciting the PTCs' periodic firing. However, the cut durations were markedly shorter (median, [25th, 75th] = 2.31s, [1.37, 3.10]s) than the PTCs' dominant periodicities. Second, it appears unlikely that the PTCs' timescales follow the content of the episode (e.g., the presence of specific characters in the movie was sparsely distributed; see Figure S6 in *ref.* 20). Further, the participants had not previously watched the episode and, therefore, could not predict the upcoming content that could, in return, dictate increase or decrease of firing activity. Lastly, if the PTCs' periodicity was modulated by the content, one would expect that the activity of PTCs with similar dominant periodicities would be similar and, thus, highly correlated in time. This was not the case in our data and the distribution of correlation coefficients between adjacent PTCs' firing (defined as PTCs with dominant periodicities within a certain time interval, e.g., 5s, 10s, 20s) was not significantly different from zero (p>0.05 for all intervals, signrank test). However, one cannot fully rule out the possibility that the neuronal firing was partly modulated by nested event boundaries of the narrative content(*28*).

Therefore, to further assess the extent to which the PTCs' periodic firing was modulated by external stimuli, we recorded data from additional five participants who watched the same episode but each half of the episode was presented to them at different speeds. In three of the participants, the first and second halves of the episode were played at regular and 1.5x speed

respectively. In the other two participants, the order of the two speeds was reversed. Of the 285 recorded units (Table S1), we identified 80 units that exhibited PTC-like behavior during both conditions (regular and faster speeds) using the methods described earlier (Methods, Electrophysiological Analyses). Of the 53 units recorded from the entorhinal cortex, 19 (35.85%) were PTCs—a percentage similar to that observed in the ten participants described previously (34.43%).

If the periodicities of PTCs were merely determined by the content of the narrative, one would expect the periodicities to change in concert with the different rates of information in the two conditions. In contrast, several PTCs maintained the dominant periodicity of their firing rate during regular- and faster-speed movie viewing (Fig. 5a). These units exhibited stable periodic behavior across the two conditions (Fig. 5b), suggesting that their periodicity was independent of the narrative content. Overall, a significant fraction of the recorded PTCs (20 of 80 total; 25.00%, [15.99, 35.94]% binomial test confidence intervals) maintained their timescales between the two conditions (Fig. 5c).

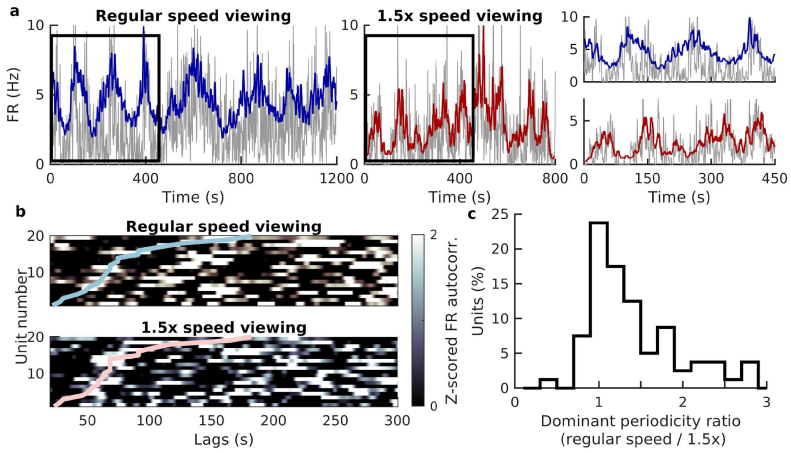

Figure 5: Maintained periodicity of PTCs during movie viewing at altered playback speeds. a. Left) Example unit's firing rate (gray) during the first half of the episode played at regular speed overlaid with the GLM-fitted firing rate (blue). Middle) Firing rate of the same unit during the second half of the episode played at 1.5x speed overlaid with GLM-fitted rate (red). Right). Zoomed in views of the unit's firing rate during the time intervals marked with black rectangles (Left and Middle). Note the same periodicity during movie viewing at regular speed (top) and accelerated speed (bottom). **b.** Z-scored firing rate autocorrelations of the units that exhibited the same periodicity during regular-speed movie viewing (top) and faster-speed movie viewing (bottom). Note that the neuron number is shared between the two panels and the colored lines represent the dominant periodicity of each unit. **c.** For each unit, the ratio of the dominant periodicity between regular-speed movie viewing and faster-speed movie viewing was computed. Shown is the distribution of this ratio across all identified PTCs (N=80). Of these PTCs, a significant percentage (25.00%, [15.99, 35.94]% binomial test) maintained their periodicity between the different speed conditions (defined as <10% change in their dominant periodicity across conditions).

<u>Remapping of PTCs' dominant periodicities during memory test</u>

Lastly, we asked whether the periodic activity related to the formation of episodic memories. We evaluated the periodic properties of PTCs during the memory test following the movie viewing (Fig. 1b). We employed the methodology described earlier to assess the significance of periodicity, as well as the dominant periods of the PTCs when participants were shown short clips and were tested for recognition memory (Methods, Behavioral Tasks). The majority (93.75%) of the PTCs that were recorded beyond the movie viewing maintained significant periodicity during the memory test, albeit at shorter timescales (Fig. 6a; Fig. S5). Although some units maintained their dominant periods during the memory test, most units (78.89%) "remapped" their periodicity to shorter timescales (Fig. 6b, c). The PTCs' shorter periodicities during the memory test was not merely a response to the clip onsets as the time between clips (median, [25th, 75th] = 4.40, [3.38, 5.44] seconds; Fig. 6c, right) was much shorter than the dominant periods observed in the PTCs (Fig. 6c, left). Overall, the PTCs' dominant periodicities

were significantly shorter during the memory test compared to movie viewing, both on a population level (Fig. 6c, p=2.64x10^{-13}, Wilcoxon ranksum test), as well as on the same cell basis (Fig. 6d; p=3.56x10^{-10}, signrank test). It is worth noting, however, that although most units reduced their dominant periods during the memory test, few PTCs within the entorhinal cortex maintained or increased their dominant periods (30.30, [15.59,48.71]%; binomial test; Fig. 6e).

Can the compression of the PTCs' timescales during the memory test be relevant for behavioral performance? To examine this, within individual participants, we computed the percentage of PTCs that remapped to shorter timescales as well as the participant's performance accuracy (the percentage of correct responses; Methods, Behavioral Tasks). The performance accuracy was positively correlated with the percentage of PTCs that compressed their timescales (Spearman p=0.046 r=0.74; Methods, Behavioral Task). The relationship between PTCs' timescale compression and memory performance was also evident for other behavioral measures such as d' given that, in our case, d' and accuracy were highly correlated (r=0.974, p=4.20x10^{-5}).

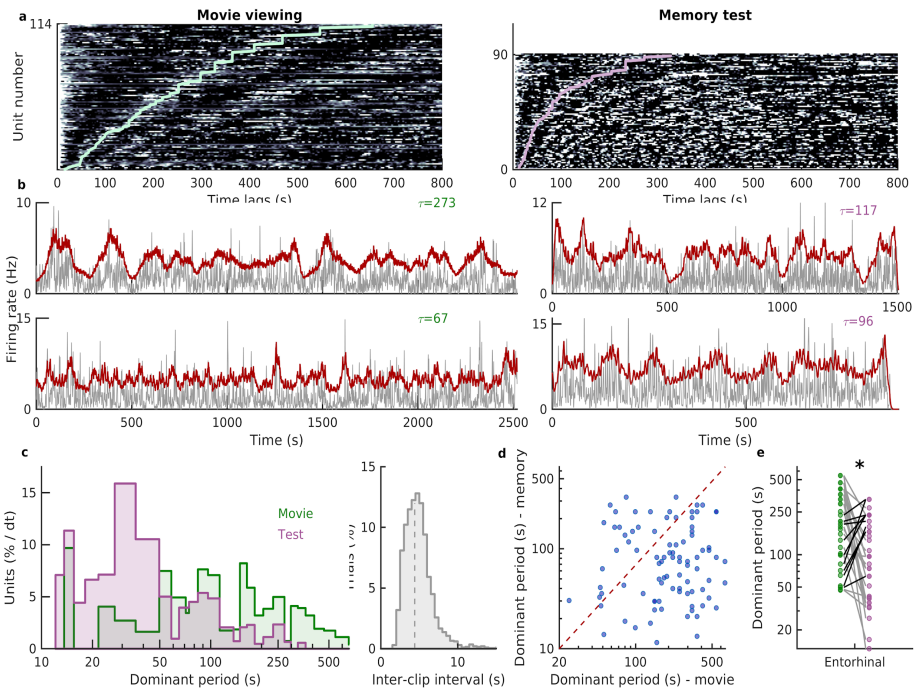

Figure 6: Periodic properties of PTCs during the memory test. **a.** Left) Z-scored autocorrelation of the PTCs' firing rate (colormap) during movie viewing sorted by the dominant periodicity (light green line) for each unit (each row)(same as Fig. 2d). Right) Same as left but for the memory test. Of the 114 PTCs recorded during movie viewing, 96 were recorded following the movie and 90 of them (93.75) remained as PTCs. **b.** Two example PTCs' firing rate during movie viewing (left) and the memory test (right) recorded from the subiculum and cingulate cortex respectively. Gray line indicates the smoothed firing rate and the red line indicates the GLM-fitted firing rate. The value tau is the dominant period of the unit in each condition. **c.** Left) The dominant periods of the units were significantly shorter (p=2.64x10^{-13}, Wilcoxon ranksum test) during memory test (n=90, purple distribution) compared to movie viewing (n=114, green histogram). Due to non-uniform time bins, the number of units per bin is normalized by the duration of the time bin. Right) The distribution of the inter-clip intervals during the memory test. Note that even the shortest dominant periods are longer than the inter-clip intervals shown here. **d.** For the same unit, the dominant period was shorter during the memory test compared to movie viewing (n=90, p= 3.56x10^{-10}, signrank test). Red dashed line indicates the diagonal. **e.** For the PTCs recorded from the entorhinal cortex, shown are the dominant periods of the same cell during movie viewing (green circles) and memory test (purple circles). Gray (black) lines correspond to the units that decreased (increased or maintained) their dominant periods. A significant percentage of the PTCs within the entorhinal cortex maintained or increased their doteminant periods during the memory test compared to movie viewing as indicated by asterisk (30.30, [15.59, 48.71]%; binomial test confidence intervals).

Discussion:

The passage of time is an integral part of human experience and, therefore, a critical dimension to consider in the investigations of human episodic memory. Recent studies in rodents have identified several cell types with time-dependent firing rates(*5–14*), notably hippocampal "time

cells”(*6*, *7*) and lateral entorhinal “ramping cells”(*14*). There have been similar quests in primate electrophysiology to discover neurons with time coding properties. The activity of temporal context cells in the monkey entorhinal cortex(*29*) align primarily with the rodent lateral entorhinal ramping cells. A recent human study employing repeating blocks of sensory inputs and required recall, described cells resembling the time and ramping cell types(*30*) . It appears that time cells and ramping cells might contribute to two distinct types of temporal information: the sequential activity of time cells can map the delays with respect to a salient event along the time axis; whereas the gradual change of activity of ramp cells in response to a salient event, which occurs at different time constants, may serve as a Laplace transformation of the elapsed time(*31*).

The time-dependent cellular machinery that we describe here is different altogether from those two cell types. It consists of a unique population of neurons with periodic modulation of activity across multiple timescales from tens of seconds to minutes. The reason that these cells so strikingly declared themselves, is likely because of the continuous uninterrupted flow of information characterizing the current study. The key property of these cells was their periodicity over nearly an hour of relatively stable context yet with enormous variability in sensory input. This stability of temporal periodicity was further demonstrated by the fact that a subset of PTCs maintained their dominant periodicity despite the change in the video playback speed. This invariance to sensory input is required from an elementary neuronal clock where temporal information can be extracted from a population of neurons that together span a rich range of temporal scales from seconds to many minutes. In fact, previous models had proposed mechanisms that involved the extraction of time from a subset of neurons with periodic properties(*25*, *26*) .

The remapping of PTCs’ periodicities seen in the memory task following movie viewing may be related to multiple factors including memory, change in the temporal structure of the task, and change in context. It might also explain why such large-scale temporal periodicity have not been reported given that the recognition portion of the task more closely resembles the traditional stimulus-response task structure often employed in the field of human electrophysiology. If the shortening of periodicity is related to memory performance, these cells may play a role in temporal compression of experience required for memory retrieval(*31*, *32*).

Of note, most of the entorhinal PTCs were in the anterior part of the entorhinal cortex. In humans, a recent fMRI study demonstrated that the activity of the anterolateral part of the entorhinal cortex is implicated in a temporal judgment memory task(*33*). Comparative anatomical studies of the human and rodent entorhinal cortex suggest that, in fact, the rodent LEC corresponds to the anterolateral portion of the entorhinal cortex and is, by nature, more multisensory compared to the MEC(*34*). Hence, it is possible that the PTCs might provide an additional temporal dimension to the incoming multisensory inputs to the entorhinal cortex.

The temporal periodicity of the periodic time cells begs comparison to spatial periodicity of grid cells. If a regular grid is a tessellation of n-dimensional Euclidean space, PTCs may be viewed then as one-dimensional temporal grid-like cells. Just like grid cells provide a multiscale map of a two-dimensional spatial environment, periodic time cells in humans may provide a multiscale map of the one-dimensional temporal environment. Akin to remapping of grid cells with change in size of the spatial environment(*15*, *35*), PTCs exhibited remapping when the temporal

structure of the task changed. Periodic time cells were by far most prevalent in entorhinal cortex, but they were also found in ~20% of anterior cingulate cells. Curiously, both entorhinal cortex and anterior cingulate were the brain regions where we had previously identified neurons with grid-like properties during human spatial navigation(*36*). Further, the entorhinal and anterior cingulate cortices were both implicated in retrospective duration estimations during encoding of long narratives(*37*).

It is possible that the periodic activity of PTCs may be related to the infra-slow (<0.1Hz) oscillations, previously described in the fMRI BOLD signals, local field potentials, as well as single unit activity(*38–42*). The reported infra-slow activity was predominantly observed in sensory and association cortices, whereas the majority of the PTCs were recorded from the entorhinal cortex. It is possible that entorhinal cortex that receives convergent inputs from these areas(*34*) may integrate such infra-slow inputs into a more robust periodic time signal.

It should be borne in mind that there might be other interpretations for our findings. First, these PTCs were observed in epilepsy patients and, thus, it cannot be ruled out that periodicity is affected by epileptogenicity. However, the majority (95%) of the PTCs in the current study were recorded from regions outside the focus of seizure onset. Second, although the periodicity of the PTCs is observed in time and it is possible to decode time from the population activity of these cells, they may be responding to other time-varying signals rendering time representation a byproduct of this process. This argument may indeed hold true even for other types of time-coding cells and may relate to a more philosophical stance on whether time exists beyond "change" and the events that occur in time (according to Aristotle and Leibniz; also see 32). Third, the periodic activity of the PTCs may subserve a range of behaviors, unrelated to time processing (e.g., chunking of experience at multiple timescales, efficient dynamics for neural communication, etc). Lastly, it is likely that PTCs have conjunctive representations along dimensions other than time—a property that, if true, bears a resemblance to the conjunctive representation of navigational variables in the entorhinal grid cells(*43*). The potential synergy of grid cells and periodic time cells in providing spatiotemporal metrics of experience, and how their input may be incorporated in the hippocampus warrant further investigation and novel paradigms.

Materials and Methods:

Participants:

Participants were 15 epilepsy patients (age = 33±10; 9 Female), implanted with intracranial depth electrodes for seizure monitoring. Informed consent as obtained prior to the surgery and experiments were done in accordance with the Institutional Review Board at UCLA. The last five participants performed an alternative version of the task.

Behavioral Tasks:

The behavioral task (programmed in PsychToolbox, Matlab) consisted of participants watching an episode of the TV series 24 (season 6, episode 1, duration ~ 42 minutes) on a laptop. Afterwards, they were presented with short clips (duration = 1.91 ± 0.72 s) and were asked to make a choice on whether they had seen the clip or not (response time duration = 2.39 ± 1.66 s), using the keyboard. The clips were divided into targets (clips chosen from episode 1 that they had just watched) and foils (clips chosen from episode 2 that they had never seen). The episodes of this series happen in consecutive hours of the day and, therefore, the characters' appearances are very similar in the target and foil clips. Further, performance accuracy for each participant was computed as follows: (TP+TN)/(TP+TN+FP+FN), where TP, TN, FP, and FN are the true positive, true negative, false positive, and false negative respectively. We also computed an alternative behavioral performance measure, specifically d' (d-prime) using the hit rate and false alarm rate values. These two measures of behavior (accuracy and d') were highly correlated (r=0.974, p=4.20x10^{-5}, Pearson correlation).

Nine out of the 10 participants performed the memory recognition test, and had extended electrophysiological recordings after the episode was over. Of these, behavioral performance data could be analyzed for eight participants. The number of presented clips, and hence the duration of the memory test, varied from participant to participant.

Five additional participants performed an alternative version of the task. They watched the same episode of the TV series 24 but, here, each half of the episode was presented at different playback speeds. In participants 1,3, and 5, the first half was presented at regular speed and the second half was presented at 1.5x speed. In participants 2 and 4, this order was reversed.

Data Acquisition:

Electrophysiological data was recorded from implanted electrodes that terminated in a set of nine 40 micro-m Platinum-Iridium microwires(*44*, *45*). The number of electrode bundles, as well as their locations, were different for each participant and determined solely by clinical criteria. Wide-band local field potentials were recorded from eight microwires (the 9th microwire was used for referencing) using a 128-channel (or 256-channel) Neuroport recording system (Blackrock Microsystems, Utah, USA) sampled at 30 kHz.

Electrode Localization:

A high-resolution post-operative CT image was obtained and co-registered to a pre-operative whole brain and high-resolution MRI for each participant using previous methods (Fig. 1c; Table S1). The location of the microelectrodes were determined by examining the location of the electrode artifact on the co-registered images. For further details, see ref. *21*.

Electrophysiological Analyses:

Data were analyzed offline using custom code as well as functions and toolboxes in Matlab and Python.

a) *Spike detection and sorting:* Spike detection and sorting was done using previous methods(*21–24*). Briefly, we applied a bandpass filter to the broadband data in the 300-3000Hz to detect spikes that were subsequently sorted using the Wave_clus toolbox. Furthermore, the automatically-detected clusters were manually inspected for: 1) spike waveforms; 2) presence of refractory spikes; as well as 3) the ISI distribution for each cluster. Clusters with firing rates below 0.05 Hz were discarded from further analysis. Note that the movie viewing and recognition memory test phases were recorded within a single session and, thus, spike detection and sorting was performed over the entire session. The activity of each unit was then separated for each phase (viewing/memory) of the experiment.

b) *Firing rates and their autocorrelations:* A time vector with a bin size of 100ms was constructed and, for each unit, the number of spikes within each time bin was computed. This raw spike train was used for the GLM analyses (next section). The smoothed spike trains were computed using a 0.5s Gaussian smoothing kernel on the raw spike histograms, which were then converted to firing rates after division by the duration of the time bin (Fig. 2a, 5a, 6b, S2, S3, S5). To inspect the presence of putative oscillations in the spiking activity, a normalized autocorrelation was computed over the smoothed firing rate.

c) *Determining significant periodic time cells:* To determine whether the periodicity in the spiking activity, as demonstrated by the autocorrelation of the firing rates, was statistically significant, we used a shuffling procedure. For each unit: 1) we chunked the firing rate into 1-second-long segments and randomly shuffled the segments in time (x 250); 2) the previous step was repeated for 2-second-long segments. This procedure yielded 500 shuffled firing rates for which an autocorrelogram was calculated. Next, we compared the autocorrelation of the true firing rate against the autocorrelation of the shuffled firing rates. Units with true autocorrelations that had values beyond the 2.5% and 97.5% of the shuffled data were identified. Further, we used a cluster-based permutation test(*46*) to correct for multiple comparisons (given the large number of lags that were being tested). Specifically, we used the function permutation_cluster_test from MNE Python package(*47*) and units with significant clusters were deemed to be periodic time cells (PTCs). The different steps of this procedure are demonstrated in Fig. S2.

d) *Generalized Linear Models (GLMs):* The time-varying firing rate of each unit was modeled as an inhomogeneous Poisson process(*48*) using basis functions that are periodic in time:

$$\lambda(t) = e^{\beta_{time} H_{time}} \cdot \frac{e^{\beta_0}}{T_{bin}}$$

$$H_{time} = \sum_i cos\frac{(2\pi t)}{T_i}$$

$$T_i \in [2{:}\,20, 30{:}\,10{:}\,300, 320{:}\,20{:}\,500]$$

Here, T_{bin} is the bin size in time (0.1 s), H refers to the design matrix associated with the temporal covariates, in this case cosine functions with different periods (T_i), and betas are the parameters associated with the design matrix in time and a constant term. Note that the exponentiation is done element-size in this case. This allowed us to determine the periods (T_i) that significantly contributed to the firing activity of the units ($p<0.001$). Oftentimes, units had more than one significant term. The distribution of these periods is shown in Fig. S1.

e) *Dominant periodicity:* To determine the strongest oscillation periodicity in the firing rate of the PTCs, we z-scored the autocorrelation of the smoothed firing rates (described in b) with respect to the shuffled data (described in c), referred to as z-scored autocorrelation for simplicity (Fig. 2d). Next, we performed FFT analysis on the z-scored autocorrelation values for each unit and the period with the maximum power was chosen as the dominant period of the unit (Fig. S2). To assess the strength of other potential periodicities, the power was normalized with respect to the strongest peak (corresponding to the dominant periodicity) and peaks with 75% of the maximum power were considered as secondary, tertiary, etc periodicities (Fig. 3).

f) *Principal Component Analysis (PCA):* We applied PCA on the activity of the PTCs (input = N x T matrix, with N=114: number of PTCs, and T= 25201: number of time bins during the movie viewing). We noted that the resulting eigenvectors appeared periodic and, thus, we computed the dominant periodicity of the eigenvectors (that described 80% of the variance) by applying an FFT and computing the period with the largest power. The distribution of the dominant periodicities of the eigenvectors were compared against shuffled data to obtain the "preferred timescales", i.e. the periods that were over-represented in the distribution. Here, the shuffled data comprised of the following: 1) constructing shuffled firing rates (input = NxT matrices); 2) applying PCA on the population of shuffled units' activity to obtain eigenvectors; 3) computing the distribution of the dominant periodicities of the shuffled eigenvectors. Steps 1-3 were repeated 250 times (Fig. S4).

g) *Decoding time from PTCs' population activity:* Decoding analysis was done using Linear Discriminant Analysis as a classification method. We divided the data into equally sized time epochs and we performed this for different bin sizes of [1:10, 15, 30, 45, 60, 90] seconds. The epoch number was used as the output of the classification model and the activity of the PTCs within each epoch was used as the input to the model. Further, we used a hold-out method, i.e. the model was trained on randomized 75% of the data and an independent 25% of the data were left aside for testing and the model performance was evaluated on the test dataset (Fig. 4). Additionally, the performance of the model was

compared against shuffled data: the same classification method was applied on the temporally shuffled activity of the PTCs. For each unit, we chunked the firing rate into 1-second-long segments and randomly shuffled them in time. We then concatenated the shuffled firing rates of all PTCs and obtained a surrogate input. We applied the same classification method on the shuffle data and computed model accuracy. We repeated this shuffling procedure 250 times.

Supplementary Materials

Fig. S1. Significant periods in the GLM-fitted firing rates.
Fig. S2. Steps to determine significant PTCs and their dominant periods.
Fig. S3. Example PTCs during movie viewing.
Fig. S4. Principal Components Analysis for the extraction of PTCs' preferred timescales.
Fig. S5. Example PTCs during movie viewing and their respective activity during the memory task.
Table S1. Electrode localizations.
Table S2. Number of total units and significant PTCs recorded per region.
Table S3. Number of PTCs recorded per participant and their timescales.

References

1. E. Tulving, *Elements of episodic memory* (Clarendon Press, 1983).

2. G. Buzsáki, R. Llinás, Space and time in the brain. *Science (80-.).* **358**, 482–485 (2017).

3. A. D. Ekstrom, C. Ranganath, Space, time, and episodic memory: The hippocampus is all over the cognitive map. *Hippocampus*. **28**, 680–687 (2018).

4. A. J. O. Dede, J. C. Frascino, J. T. Wixted, L. R. Squire, Learning and remembering real-world events after medial temporal lobe damage. *Proc. Natl. Acad. Sci.* **113**, 13480–13485 (2016).

5. E. Pastalkova, V. Itskov, A. Amarasingham, G. Buzsaki, Internally Generated Cell Assembly Sequences in the Rat Hippocampus. *Science (80-.).* **321**, 1322–1327 (2008).

6. C. J. MacDonald, K. Q. Lepage, U. T. Eden, H. Eichenbaum, Hippocampal "Time Cells" Bridge the Gap in Memory for Discontiguous Events. *Neuron*. **71**, 737–749 (2011).

7. B. J. Kraus, M. P. Brandon, R. J. Robinson, M. A. Connerney, M. E. Hasselmo, H. Eichenbaum, During Running in Place, Grid Cells Integrate Elapsed Time and Distance Run. *Neuron*. **88**, 578–589 (2015).

8. W. Mau, D. W. Sullivan, N. R. Kinsky, M. E. Hasselmo, M. W. Howard, H. Eichenbaum, The Same Hippocampal CA1 Population Simultaneously Codes Temporal Information over Multiple Timescales. *Curr. Biol.* **28**, 1499-1508.e4 (2018).

9. J. R. Manns, M. W. Howard, H. Eichenbaum, Gradual Changes in Hippocampal Activity Support Remembering the Order of Events. *Neuron*. **56**, 530–540 (2007).

10. E. A. Mankin, F. T. Sparks, B. Slayyeh, R. J. Sutherland, S. Leutgeb, J. K. Leutgeb, Neuronal code for extended time in the hippocampus. *Proc. Natl. Acad. Sci. U. S. A.* **109**, 19462–7 (2012).

11. E. A. Mankin, G. W. Diehl, F. T. Sparks, S. Leutgeb, J. K. Leutgeb, Hippocampal CA2 Activity Patterns Change over Time to a Larger Extent than between Spatial Contexts. *Neuron*. **85**, 190–201 (2015).

12. C. Sun, W. Yang, J. Martin, S. Tonegawa, Hippocampal neurons represent events as transferable units of experience. *Nat. Neurosci.* **23**, 651–663 (2020).

13. A. Tsao, M.-B. Moser, E. I. Moser, Traces of Experience in the Lateral Entorhinal Cortex. *Curr. Biol.* **23**, 399–405 (2013).

14. A. Tsao, J. Sugar, L. Lu, C. Wang, J. J. Knierim, M.-B. Moser, E. I. Moser, Integrating time from experience in the lateral entorhinal cortex. *Nature*. **561**, 57–62 (2018).

15. T. Hafting, M. Fyhn, S. Molden, M.-B. Moser, E. I. Moser, Microstructure of a spatial map in the entorhinal cortex. *Nature*. **436**, 801–806 (2005).

16. H. Stensola, T. Stensola, T. Solstad, K. FrØland, M. B. Moser, E. I. Moser, The entorhinal grid map is discretized. *Nature*. **492** (2012), pp. 72–78.

17. J. G. Heys, D. A. Dombeck, Evidence for a subcircuit in medial entorhinal cortex representing elapsed time during immobility. *Nat. Neurosci.* **21**, 1574–1582 (2018).

18. J. B. Issa, G. Tocker, M. E. Hasselmo, J. G. Heys, D. A. Dombeck, Navigating Through Time: A Spatial Navigation Perspective on How the Brain May Encode Time. *Annu. Rev. Neurosci.* **43**, 73–93 (2020).

19. J. G. Heys, Z. Wu, A. L. Allegra Mascaro, D. A. Dombeck, Inactivation of the Medial Entorhinal Cortex Selectively Disrupts Learning of Interval Timing. *Cell Rep.* **32**, 108163 (2020).

20. H. Tang, J. Singer, M. J. Ison, G. Pivazyan, M. Romaine, R. Frias, E. Meller, A. Boulin, J. Carroll, V. Perron, S. Dowcett, M. Arellano, G. Kreiman, Predicting episodic memory formation for movie events. *Sci. Rep.* **6**, 30175 (2016).

21. N. A. Suthana, N. N. Parikshak, A. D. Ekstrom, M. J. Ison, B. J. Knowlton, S. Y. Bookheimer, I. Fried, Specific responses of human hippocampal neurons are associated with better memory. *Proc. Natl. Acad. Sci. U. S. A.* **112**, 10503–8 (2015).

22. R. Q. Quiroga, L. Reddy, G. Kreiman, C. Koch, I. Fried, Invariant visual representation by single neurons in the human brain. *Nature*. **435**, 1102–1107 (2005).

23. R. Q. Quiroga, Z. Nadasdy, Y. Ben-Shaul, Unsupervised Spike Detection and Sorting with Wavelets and Superparamagnetic Clustering. *Neural Comput.* **16**, 1661–1687 (2004).

24. M. J. J. Ison, R. Quian Quiroga, I. Fried, R. Quian Quiroga, I. Fried, Rapid Encoding of New Memories by Individual Neurons in the Human Brain. *Neuron*. **87**, 220–230 (2015).

25. E. T. Rolls, P. Mills, The Generation of Time in the Hippocampal Memory System. *Cell Rep.* **28**, 1649-1658.e6 (2019).

26. S. Teki, B.-M. Gu, W. H. Meck, The persistence of memory: how the brain encodes time in memory. *Curr. Opin. Behav. Sci.* **17**, 178–185 (2017).

27. T. Solstad, E. I. Moser, G. T. Einevoll, From grid cells to place cells: A mathematical model. *Hippocampus*. **16**, 1026–1031 (2006).

28. C. Baldassano, J. Chen, A. Zadbood, J. W. Pillow, U. Hasson, K. A. Norman, Discovering Event Structure in Continuous Narrative Perception and Memory. *Neuron*. **95**, 709-721.e5 (2017).

29. I. M. Bright, M. L. R. Meister, N. A. Cruzado, Z. Tiganj, E. A. Buffalo, M. W. Howard, A temporal record of the past with a spectrum of time constants in the monkey entorhinal cortex. *Proc. Natl. Acad. Sci. U. S. A.* (2020), doi:10.1073/pnas.1917197117.

30. G. Umbach, P. Kantak, J. Jacobs, M. Kahana, B. E. Pfeiffer, M. Sperling, B. Lega, Time cells in the human hippocampus and entorhinal cortex support episodic memory. *Proc. Natl. Acad. Sci. U. S. A.* **117**, 28463–28474 (2020).

31. M. W. Howard, Memory as Perception of the Past: Compressed Time inMind and Brain. *Trends Cogn. Sci.* **22**, 124–136 (2018).

32. G. Buzsáki, D. Tingley, Space and Time: The Hippocampus as a Sequence Generator. *Trends Cogn. Sci.* **22**, 853–869 (2018).

33. M. E. Montchal, Z. M. Reagh, M. A. Yassa, Precise temporal memories are supported by the lateral entorhinal cortex in humans. *Nat. Neurosci.* **22**, 284–288 (2019).

34. T. P. Doan, M. J. Lagartos-Donate, E. S. Nilssen, S. Ohara, M. P. Witter, Convergent Projections from Perirhinal and Postrhinal Cortices Suggest a Multisensory Nature of Lateral, but Not Medial, Entorhinal Cortex. *Cell Rep.* **29**, 617-627.e7 (2019).

35. J. D. Monaco, L. F. Abbott, L. F. Abbott, Modular Realignment of Entorhinal Grid Cell Activity as a Basis for Hippocampal Remapping. *J. Neurosci.* **31**, 9414–9425 (2011).

36. J. F. Miller, M. Neufang, A. Solway, A. Brandt, M. Trippel, I. Mader, S. Hefft, M. Merkow, S. M. Polyn, J. Jacobs, M. J. Kahana, A. Schulze-Bonhage, Neural activity in human hippocampal formation reveals the spatial context of retrieved memories. *Science*. **342**, 1111–4 (2013).

37. O. Lositsky, J. Chen, D. Toker, C. J. Honey, M. Shvartsman, J. L. Poppenk, U. Hasson, K. A. Norman, Neural pattern change during encoding of a narrative predicts retrospective duration estimates. *Elife*. **5** (2016), doi:10.7554/eLife.16070.

38. Y. Nir, R. Mukamel, I. Dinstein, E. Privman, M. Harel, L. Fisch, H. Gelbard-Sagiv, S. Kipervasser, F. Andelman, M. Y. Neufeld, U. Kramer, A. Arieli, I. Fried, R. Malach, Interhemispheric correlations of slow spontaneous neuronal fluctuations revealed in human sensory cortex. *Nat. Neurosci.* **11**, 1100–1108 (2008).

39. M. Steriade, A. Nuñez, F. Amzica, A novel slow (< 1 Hz) oscillation of neocortical neurons in vivo: depolarizing and hyperpolarizing components. *J. Neurosci.* **13**, 3252–65 (1993).

40. D. A. Leopold, Y. Murayama, N. K. Logothetis, Very Slow Activity Fluctuations in Monkey Visual Cortex: Implications for Functional Brain Imaging. *Cereb. Cortex*. **13**, 422–433 (2003).

41. J. M. Palva, S. Palva, Infra-slow fluctuations in electrophysiological recordings, blood-oxygenation-level-dependent signals, and psychophysical time series. *Neuroimage*. **62**, 2201–11 (2012).

42. N. A. Aladjalova, Infra-slow rhythmic oscillations of the steady potential of the cerebral cortex. *Nature*. **179** (1957), pp. 957–959.

43. F. Sargolini, M. Fyhn, T. Hafting, B. L. McNaughton, M. P. Witter, M.-B. Moser, E. I. Moser, Conjunctive representation of position, direction, and velocity in entorhinal cortex. *Science*. **312**, 758–62 (2006).

44. I. Fried, K. A. MacDonald, C. L. Wilson, Single Neuron Activity in Human Hippocampus and Amygdala during Recognition of Faces and Objects. *Neuron*. **18**, 753–765 (1997).

45. I. Fried, C. L. Wilson, N. T. Maidment, J. Engel, E. Behnke, T. A. Fields, K. A. Macdonald, J. W. Morrow, L. Ackerson, Cerebral microdialysis combined with single-neuron and electroencephalographic recording in neurosurgical patients: Technical note. *J. Neurosurg.* **91**, 697–705 (1999).

46. E. Maris, R. Oostenveld, Nonparametric statistical testing of EEG- and MEG-data. *J. Neurosci. Methods*. **164**, 177–190 (2007).

47. A. Gramfort, M. Luessi, E. Larson, D. A. Engemann, D. Strohmeier, C. Brodbeck, R. Goj, M. Jas, T. Brooks, L. Parkkonen, M. Hämäläinen, MEG and EEG data analysis with MNE-Python. *Front. Neurosci.* (2013), doi:10.3389/fnins.2013.00267.

48. L. Acharya, Z. M. Aghajan, C. Vuong, J. J. Moore, M. R. Mehta, Causal Influence of Visual Cues on Hippocampal Directional Selectivity. *Cell*. **164**, 197–207 (2016).

Acknowledgments

General: We thank Matias Ison, Hanlin Tang, Jie Zheng, and Guldamla Kalender for assistance with data collection and processing. We also thank the participants for taking part in our study.

Funding: This work was supported by the NIH NINDS (NS033221 and NS084017 to I.F.) and NSF Center for Brains, Minds and Machines and McKnight Foundation (G.K.)

Author Contributions: Z.M.A., G.K., and I.F. conceived and designed the research. Z.M.A. and I.F. performed analyses. I.F. performed all implantation of the depth electrodes. Z.M.A. and I.F. wrote the paper. All the authors commented on the manuscript.

Competing interests: Authors declare no competing interests.

Data and materials availability: Custom code used and datasets analyzed for the current study are available from the corresponding author upon reasonable request.

Figures and Tables

For ease of readability, we have included the main figures and legends within the text.

Supplementary Materials

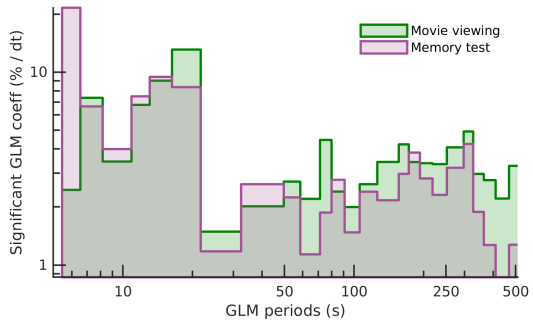

Fig. S1. Significant periods in the GLM-fitted firing rates.

The distribution of the periods that were deemed significant ($p<0.001$) in describing the time-varying firing rate of the units during movie viewing (green; number of significant periods detected by the GLM method = 1335 from 114 units) and memory test (purple; N = 685 from 90 units). For the majority of the units, the GLM fitting resulted in more than one term that contributed to the firing. Note the shift towards shorter periodicities during the memory test compared to the movie viewing ($p=1.16\text{x}10^{-7}$; Wilcoxon ranksum test).

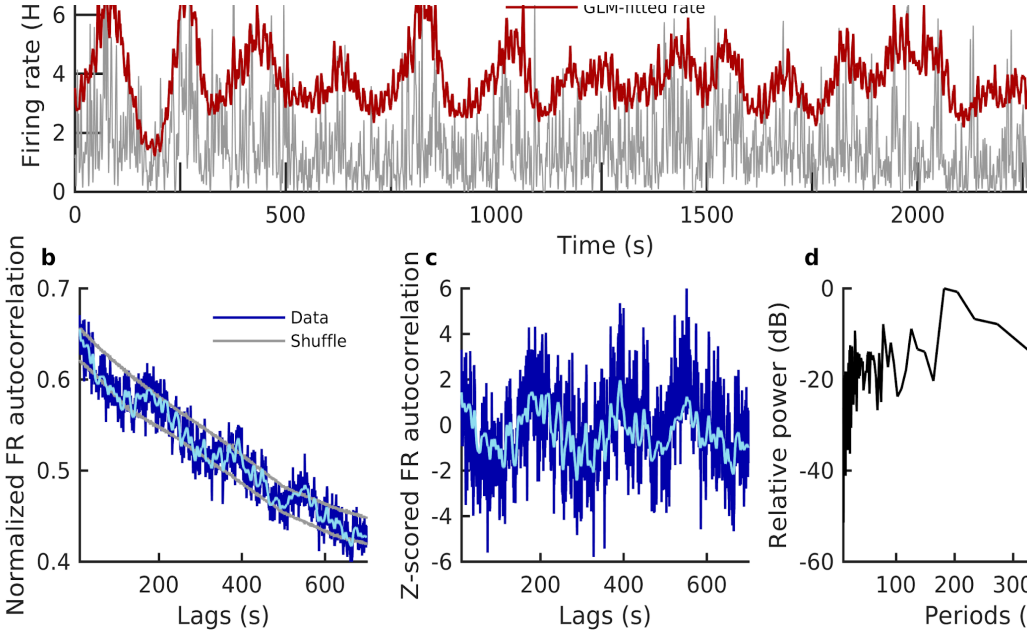

Fig. S2. Steps to determine significant PTCs and their dominant periods.

a. Example PTC from the left entorhinal cortex; smoothed firing rate (gray) overlaid with the GLM-fitted rate (red). **b.** Normalized autocorrelation of the smoothed firing rate shown in (a) is shown in dark blue. Gray lines indicate the 2.5% and 97.5% of the shuffle data (see Methods, Electrophysiological Analyses), which were obtained from generating shuffled firing rates, followed by computing the autocorrelograms of the shuffled rates. A unit with firing rate autocorrelations beyond the shuffled data was then corrected for multiple comparisons (using cluster based permutation test), and units with significant clusters were deemed to be PTCs. **c.** The true firing rate autocorrelogram was z-scored with respect to the shuffled data (subtracting the mean and division by the standard deviation) and is shown in dark blue (light blue curve is the smoothed version of the z-scored autocorrelation and is shown only for visualization purposes). **d.** Relative power (FFT normalized by the maximum power) of the z-scored firing rate autocorrelogram (c), which was used to compute the dominant periodicity of the units' firing rates. Dominant periodicity was defined as the period that contained the maximum power (~200s for this unit).

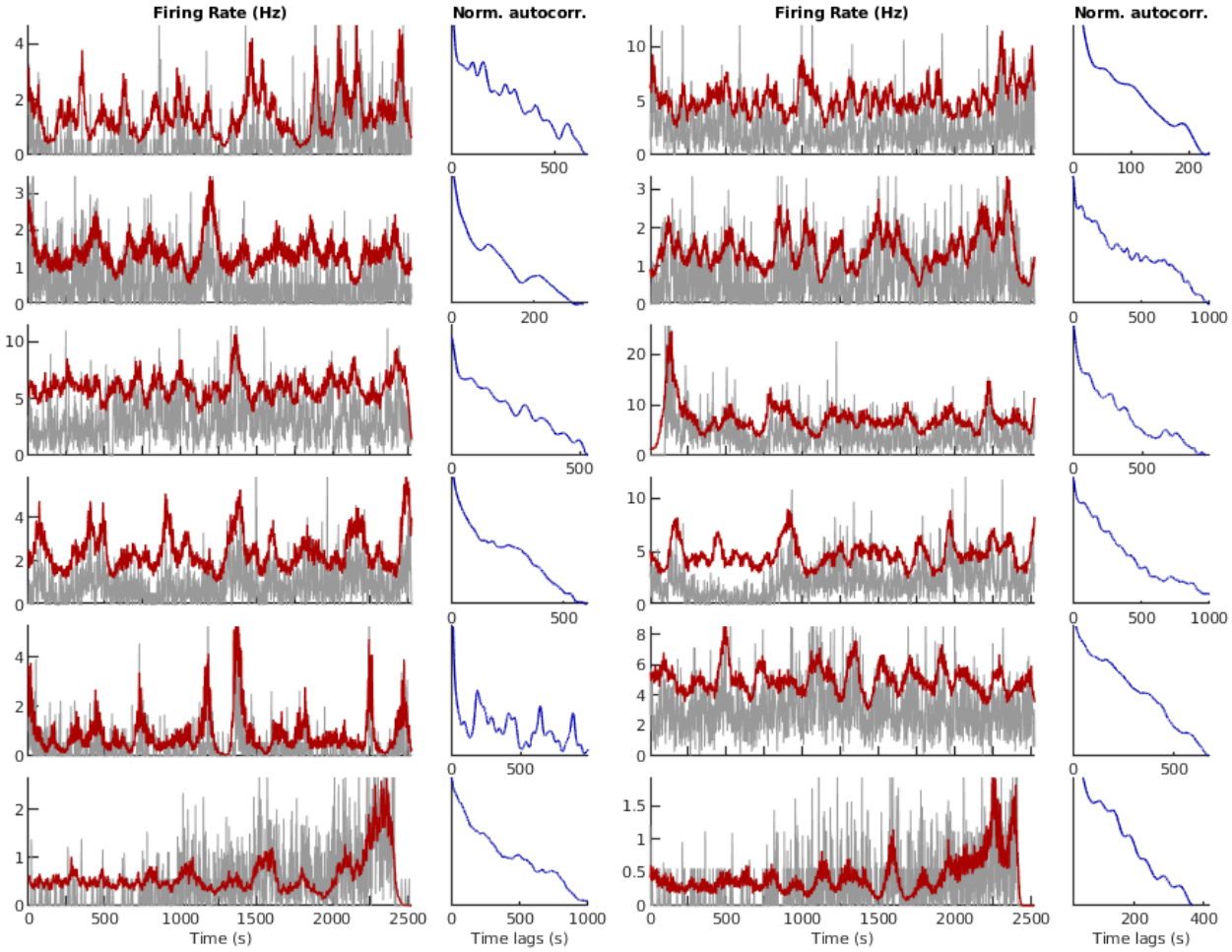

Fig. S3. Example PTCs during movie viewing.

Additional 12 units that were identified as PTCs. Within each column: Left) Smoothed firing rate (gray) overlaid with GLM-fitted rate (red); Right) Normalized autocorrelation of the smoothed firing rate to demonstrate periodicity. These units were recorded from the following regions (from left to right within the rows): Mid. Post. Cingulate; Entorhinal; Entorhinal; Amygdala; Entorhinal; vm-PFC; Parahippocampal Gyrus; Entorhinal; Occipital: Entorhinal; Entorhinal; Entorhinal.

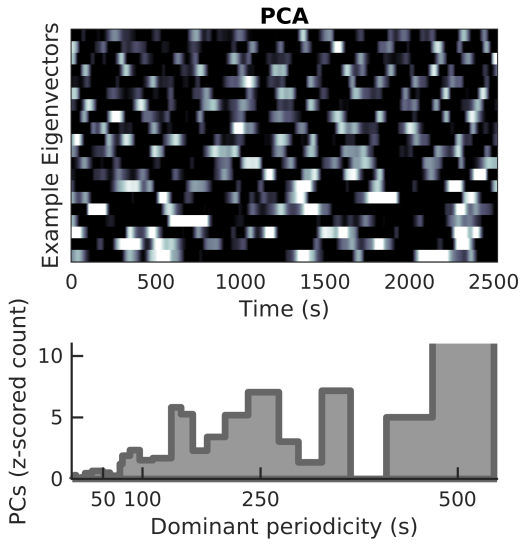

Fig. S4. Principal Components Analysis for the extraction of PTCs' preferred timescales. Top) Example (smoothed) eigenvectors obtained from applying principal component analysis on the population of the PTCs' firing rates. The eigenvectors themselves appeared periodic in time. Bottom) The distribution of the dominant periodicity of the PCA eigenvectors (that explained 80% of the variance data) was z-scored with respect to the shuffled data (Methods, Electrophysiological Analyses). Note the periods that are over-represented (preferred timescales) in the distribution, which are consistent with the timescales shown in Fig. 3c.

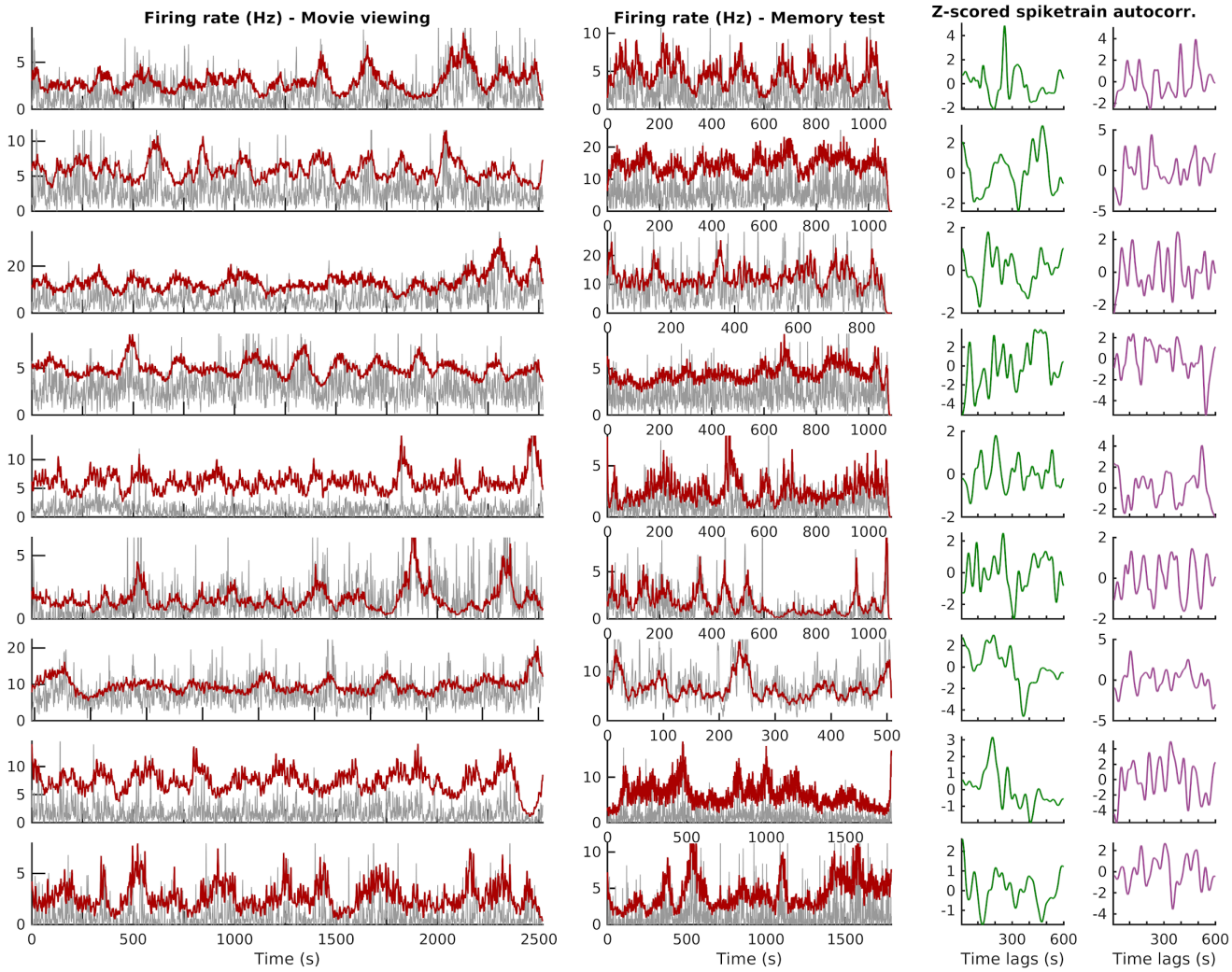

Fig. S5. Example PTCs during movie viewing and their respective activity during the memory task.

We tracked the activity of the same unit during movie viewing and memory test. Shown are nine different units (each row). Left) Firing rate (gray) and GLM-fitted rate (red) during movie viewing. Middle) Same as in (left) but during the memory test. Right) Z-scored autocorrelograms of the spike trains (smoothed only for visualization purposes) during movie viewing (green) and memory test (purple). These units were recorded from the following regions (top to bottom): Entorhinal; Entorhinal; Superior Temporal; Entorhinal; Amygdala; A. Cingulate; Entorhinal; Entorhinal; Entorhinal. Note the higher frequency oscillations (faster periodicity) during memory test (purple).

Locs Pt. ID	Entorhinal Cortex	Hippocampus	Parahippocampal Gyrus	Subiculum	Amygdala	Superior Temporal Gyrus	Anterior Cingulate	Middle & Posterior Cingulate	Ventromedial Prefrontal Cortex	PreSMA	Occipital	Insula
1	-	R	-	-	R	L R (2)	-	L R (3)	-	-	-	-
2	L R	-	L	R	-	-	L R (2)	R	L	L R	-	-
3	L	-	L R	L	-	-	-	-	-	-	L (2) R	-
4	L R (2)	L	-	-	L R	-	L R	-	L R	L R	-	-
5	L	-	-	L	L	-	-	-	L	-	-	-
6	R	L	R	-	L R	-	R	-	-	-	-	-
7	L R	L R	R	-	L R	-	-	-	-	-	-	-
8	L R	R	-	-	L R	-	L R	-	R	L R	-	-
9	L R	L R	-	-	L	-	L R	-	L R	-	-	-
10	L R	-	-	L R	R	R	R	-	L	-	R	-
11[a]	-	R	-	L	L	L	L	-	R L	R	L	L
12	R	R	-	-	L	-	-	-	-	-	-	R (2) L
13	R L	R L	-	-	L	L	-	-	L	-	-	-
14	L	R L	R	-	L	R	-	-	R	-	-	-
15	R L	R L	-	-	L	L	R L	-	R	-	-	-

Table S1. Electrode localizations.

For each participant (rows), all of the recording electrode locations that had units are listed (columns: categories that were used for group analysis). The hemispheric location of the electrodes are marked with R and L, referring to the right and left hemispheres respectively. The numbers in parentheses indicate the number of electrodes within each hemisphere (if there were more than one). [a] Additional units were recorded in the fusiform gyrus. Participants 11-15

performed an alternative version of the task that consisted of watching one half of the episode at regular speed and the other half at a faster speed (1.5x speed; see Methods).

Participant	Number of Units	Number of PTCs
Hippocampus	26	4
Subiculum	12	1
Entorhinal Cortex	122	42
Parahippocampal	27	8
Amygdala	94	15
Superior Temporal	35	6
Anterior Cingulate	63	14
Middle & Posterior Cingulate	44	6
VM Prefrontal Cortex	41	7
PreSMA	25	3
Occipital	48	8

Table S2. Number of total units and significant PTCs recorded per region.
The numbers reported here are from the original 10 participants.

Participant	Number of PTCs	PTCs' timescales (s) mean dominant period ± std
1	14	190.04±108.43
2	18	277.26±191.59
3	10	229.73±112.57
4	22	228.53±156.99
5	1	131.10±0.00
6	5	209.90±213.12
7	8	186.55±128.28
8	7	186.82±103.19
9	24	313.43±184.74
10	5	348.49±89.64

Table S3. Number of PTCs recorded per participant and their timescales.
The numbers reported here are from the original 10 participants. PTCs' timescales are represented by their dominant periodicities (shown are mean ± std within each participant).